

Shell Cross-Linked Knedels: A Synthetic Study of the Factors Affecting the Dimensions and Properties of Amphiphilic Core-Shell Nanospheres

K. Bruce Thurmond, II, Tomasz Kowalewski, and Karen L. Wooley*

Contribution from the Department of Chemistry, Washington University, One Brookings Drive, St. Louis, Missouri 63130-4899

Received April 3, 1997[⊗]

Abstract: Shell cross-linked knedels (SCK's), nanometer-sized spherical particles that are composed of a core-shell morphology, were prepared by intramolecular polymerization of side chain functionalities along the backbone of the hydrophilic block of amphiphilic polystyrene-*b*-poly(vinylpyridine) block copolymers organized into micellar assemblies. Control over the size of the SCK's was demonstrated through variation of the chemistry and processing conditions. The solid-state SCK diameters (from atomic force microscopy) ranged from 8 to 30 nm, depending upon the chemical composition and micellization time. The relative amount and nature of hydrophilicity in the amphiphilic block copolymer precursor to the SCK's affects the propensity for aggregation, leading to differences in the aggregation numbers of polymer chains within the micelles and to differences in the dimensions of the SCK's. Therefore, increased lengths of the PS (hydrophobic) block in comparison to the PVP (hydrophilic) block gave larger aggregation numbers and larger SCK's. Alternatively, the incorporation of more quaternized sites along the PVP backbone (increased hydrophilicity) gave smaller SCK's. Quaternization of the PVP using poly(ethylene oxide) (PEO) to give water soluble side chain grafts also resulted in decreased SCK diameters and more narrow size distributions, in comparison to the SCK with no PEO. Allowing longer times for micelle formation prior to cross-linking gave larger SCK's and broader size distributions, due to coalescence of the polymer micelles.

Introduction

The development of new polymer structures and architectures has become an intensely studied field of nanotechnology. This is due to both academic interests, and, more importantly, the potential that unique nanometer-sized structures have shown toward performance in a broad range of medical, mechanical, and electronic applications.^{1–7} The properties of macromolecules and macromolecular assemblies are affected by their sizes and shapes; thus a great deal of effort has been directed toward controlling the geometries of individual polymers and larger aggregates. Chemical functionality, physical means, and self-assembly are techniques that have been used to generate an array of shaped structures. For example, taking advantage of the selective chemical functionality and reactivity of multifunctional monomers allows for polymer growth through specific sites to produce dendritic or hyperbranched polymers,⁸ which are two forms of globular macromolecules. Templating,^{4,9} micromolding,⁵ and capillary action⁶ are techniques that have been used to provide structural control in the nanofabrication of large and complex patterns of materials through physical manipulation. Similarly, self-organization, driven by attractive and/or repulsive

forces, has provided a powerful and simple method for the creation of unique structural assemblies.^{10–19}

Polymer micelles are amphiphilic particles with diameters generally ranging from 20 to 200 nm that are formed through the self-assembly of block copolymers.^{13,14,20,21} Polymer micelles are being actively investigated for a number of potential applications that would take advantage of their core-shell structure; for example, they are showing promise as vehicles for drug delivery.^{1,3} Micelles exist at concentrations above a critical micelle concentration (cmc), and the structure of the micelle is dependent upon the nature of the solvent system. In general, micelles are thought to have a hydrophobic core with a hydrophilic shell, but if the solvent system is made less hydrophilic, then the core and the shell may be inverted to give reverse micelles. These limitations on environment specificity can become problematic when working with polymer micelles.

Polymer micelles are typically spherical in shape, but several morphologies have been reported for at least two different block

[⊗] Abstract published in *Advance ACS Abstracts*, July 1, 1997.

(1) Gref, R.; Minamitake, Y.; Peracchia, M. T.; Trubetskoy, V.; Torchilin, V.; Langer, R. *Science* **1994**, *263*, 1600.

(2) Parthasarathy, R. V.; Martin, C. R. *Nature* **1994**, *369*, 298.

(3) Kataoka, K.; Kwon, G. S.; Yokoyama, M.; Okano, T.; Sakurai, Y. *J. Controlled Release* **1993**, *24*, 119.

(4) Martin, C. *Science* **1994**, *266*, 1961.

(5) Xia, Y.; Kim, E.; Zhao, X. M.; Rogers, J. A.; Prentiss, M.; Whitesides, G. *Science* **1996**, *273*, 347.

(6) Kim, E.; Xia, Y.; Whitesides, G. M. *Adv. Mater.* **1996**, *8* (3), 245.

(7) Stupp, S. I.; Son, S.; Lin, H. C.; Li, L. S. *Science* **1993**, *259*, 59.

(8) *Advances in Dendritic Macromolecules*; Newkome, G. R., Ed.; JAI Press: Greenwich, CT, 1994, 1995; Vols. 1–2.

(9) Evans, E.; Bowman, H.; Leung, A.; Needham, D.; Tirrell, D. *Science* **1996**, *273*, 933.

(10) Guo, A.; Liu, G.; Tao, J. *Macromolecules* **1996**, *29* (7), 2487.

(11) Ishizu, K.; Saito, R. *Polym.-Plast. Technol. Eng.* **1992**, *31* (7 and 8), 607.

(12) Ishizu, K.; Fukutomi, T. *J. Polym. Sci.: Part C: Polym. Lett* **1988**, *26*, 281.

(13) Zhang, L.; Eisenberg, A. *Science* **1995**, *268*, 1728.

(14) Qin, A.; Tian, M.; Ramireddy, C.; Webber, S. E.; Munk, P.; Tuzar, Z. *Macromolecules* **1994**, *27*, 120.

(15) Percec, V.; Schlueter, D.; Ronda, J. C.; Johansson, G.; Ungar, G.; Zhou, J. P. *Macromolecules* **1996**, *29*, 1464.

(16) Ghadiri, M. R.; Granja, J. R.; Milligan, R. A.; McRee, D. E.; Khazanovich, N. *Nature* **1993**, *366*, 324.

(17) Stupp, S. I.; Son, S.; Li, H. C.; Keser, M. *J. Am. Chem. Soc.* **1995**, *117*, 5212.

(18) Percec, V.; Johansson, G.; Ungar, G.; Zhou, J. *J. Amer. Chem. Soc.* **1996**, *118*, 9855.

(19) Ringsdorf, H.; Schlarb, B.; Venzmer, J. *Angew. Chem., Int. Ed. Engl.* **1988**, *27*, 113.

(20) Astafieva, I.; Zhong, X. F.; Eisenberg, A. *Macromolecules* **1993**, *26*, 7339.

(21) Wilhelm, M.; Zhao, C. L.; Wang, Y.; Xu, R.; Winnik, M. A.; Mura, J. L.; Riess, G.; Croucher, M. D. *Macromolecules* **1991**, *24*, 1033.

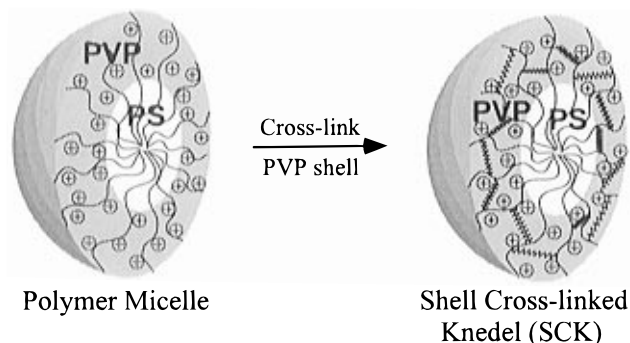


Figure 1. Schematic representation of the formation of SCK's.

copolymers through variations in the block length ratios, thus making it possible to obtain a broad range of particle shapes and sizes.¹³ Since applications are size specific, the particle size for any type of nanostructure is a crucial parameter that must be accounted for when attempting to apply these synthetic materials. For example, the efficiency of DNA transfection using polyamidoamine (PAMAM) dendrimers as the delivery agent was found to be highly dependent upon the generation number (i.e. dendrimer size).^{22–25} The ability to complex or encapsulate guest materials has also been shown to be reliant on the relative size of the guest and host.^{26,27}

We recently reported²⁸ a method for the formation of shell cross-linked knedels²⁹ (SCK's) as a novel polymer micelle structure,³⁰ which is stabilized through covalent bonds between functionalities along the backbone of polymer chains located in the peripheral shell. The initial SCK's had average diameters of ~22 nm, which is intermediate between the accessible sizes for dendrimers and latex particles, making unique properties and applications possible for SCK's. Herein, we report several parameters that affect the SCK sizes and variations in SCK compositions, as well as the ability to control these properties.

Results and Discussion

As shown schematically in Figure 1, the SCK's are prepared by cross-linking of functionalities located in the shell domain of polymer micelles. The first example of an SCK was composed of a hydrophobic polystyrene (PS) core and a hydrophilic cross-linked poly(vinylpyridine) (PVP) shell, which was prepared by a three-step process. Initially, a block copolymer consisting of polystyrene and poly(vinylpyridine) is synthesized through anionic "living" polymerization (Scheme 1). Secondly, quaternization of a percentage of the available pyridyl groups with *p*-(chloromethyl)styrene imparts an am-

phiphilic nature to the block copolymer and also introduces the cross-linkable moiety. Micelle formation is then accomplished by dissolving the quaternized block copolymer in a mixture of water and tetrahydrofuran (THF). Finally, the resulting micelle is cross-linked by irradiation in a Rayonet photochemical reactor (Hg lamps) in the presence of a radical initiator³¹ to produce the shell cross-linked knedel (SCK) (Figure 1 and Scheme 1). In order to improve the understanding of SCK formation, and to generate materials of a broader range of sizes, variation in the chemical composition of the amphiphilic block copolymers and the reaction conditions used for SCK formation were investigated (Table 1). Characterization of the resulting effects upon the SCK sizes and shapes were evaluated by atomic force microscopy (AFM).

Similar to light-scattering techniques, AFM provides measurement of size and size distribution. Importantly, AFM also allows for visualization of three-dimensional shape²⁸ and measurement of sizes in the solid state, which eliminates perturbations due to solvent swelling. In the previous study,²⁸ AFM was used to establish that SCK's are able to form monolayers of aggregates upon adsorption on freshly cleaved mica, indicating that the cross-linking of the shell proceeds through intramicellar reactions. Monolayer aggregates of SCK's exhibited uniform heights from the center to the edge, and the heights and lateral sizes of SCK's in those aggregates agreed to within 10%, indicating little or no flattening of the SCK's upon adsorption onto the surface of mica. These observations validated the use of heights of isolated SCK's, deposited from dilute solutions, as a measure of the unperturbed particle sizes. As discussed below, single-particle analysis allows for the determination of particle size distributions, providing more adequate characterization of the materials.

Relative Block Lengths. The effects of the relative ratios of hydrophobic and hydrophilic block lengths upon the resulting SCK's were determined from block copolymers having three different PS:PVP contents. The block copolymers used for this study were prepared by anionic polymerization and contained PS:PVP ratios of 1:2.0, 1:1.2, and 1.9:1 giving **1**, **2**, and **3**, respectively (Scheme 1). Quaternization of ~45% of the available pyridyl groups of **1–3** with *p*-(chloromethyl)styrene gave the amphiphilic block copolymers **4–6**. Each of the quaternized block copolymers **4–6**, was soluble in the H₂O:THF, 2.5:1 solvent mixture, which provided an environment for self-assembly into spherical micellar aggregates at block copolymer concentrations of ~10⁻⁵ M. Irradiation of the polymer micelle solutions of **4–6** containing 4,4'-azobis(4-cyanovaleric acid)³¹ formed the SCK's **7–9**, respectively, as demonstrated by the elimination of a detectable cmc by pyrene excitation spectroscopy.^{21,28}

The first apparent difference between the SCK's **7–9**, was observed as differing qualitative degrees of solubility. The SCK composed of 1:2.0 PS:PVP, **7**, remained suspended in the aqueous solution for an indefinite period of time even after removal of THF, while **8** began to precipitate after a month under the same conditions. Furthermore, **9**, which is composed of the highest hydrophobic content, with a 1.9:1 ratio of PS:PVP, was visually a more turbid solution than either **7** or **8** immediately following cross-linking.

(22) Kukowska-Latallo, J. F.; Bielinska, A. U.; Johnson, J.; Spindler, R.; Tomalia, D. A.; Baker Jr., J. R. *Proc. Natl. Acad. Sci. U.S.A.* **1996**, *93*, 4897.

(23) Bielinska, A. U.; Kukowska-Latallo, J.; Piehler, L. T.; Tomalia, D. A.; Spindler, R.; Yin, R.; Baker Jr.; J. R. *Polym. Mater. Sci. Eng.* **1995**, *73*, 273.

(24) Haensler, J.; Szoka Jr., F. C. *Bioconjugate Chem.* **1993**, *4*, 372.

(25) Baker, J. R., Jr.; Bielinska, A.; Johnson, J.; Yin, R.; Kukowska-Latallo, J. F. *Artificial Self-Assembling Systems for Gene Delivery*, Felgner, P. L., Heller, M. J., Lehn, P., Behr, J. P., Szoka, F. C., Jr., Eds.; American Chemical Society: Washington, DC, 1996; pp 129–145.

(26) Wolfert, M. A.; Seymour, L. W. *Gene Ther.* **1996**, *3*, 269.

(27) Stevelmans, S.; van Hest, J. C. M.; Jansen, J. F. G. A.; van Bostel, D. A. F. J.; de Brabander-van den Berg, E. M. M.; Meijer, E. W. *J. Am. Chem. Soc.* **1996**, *118*, 7398.

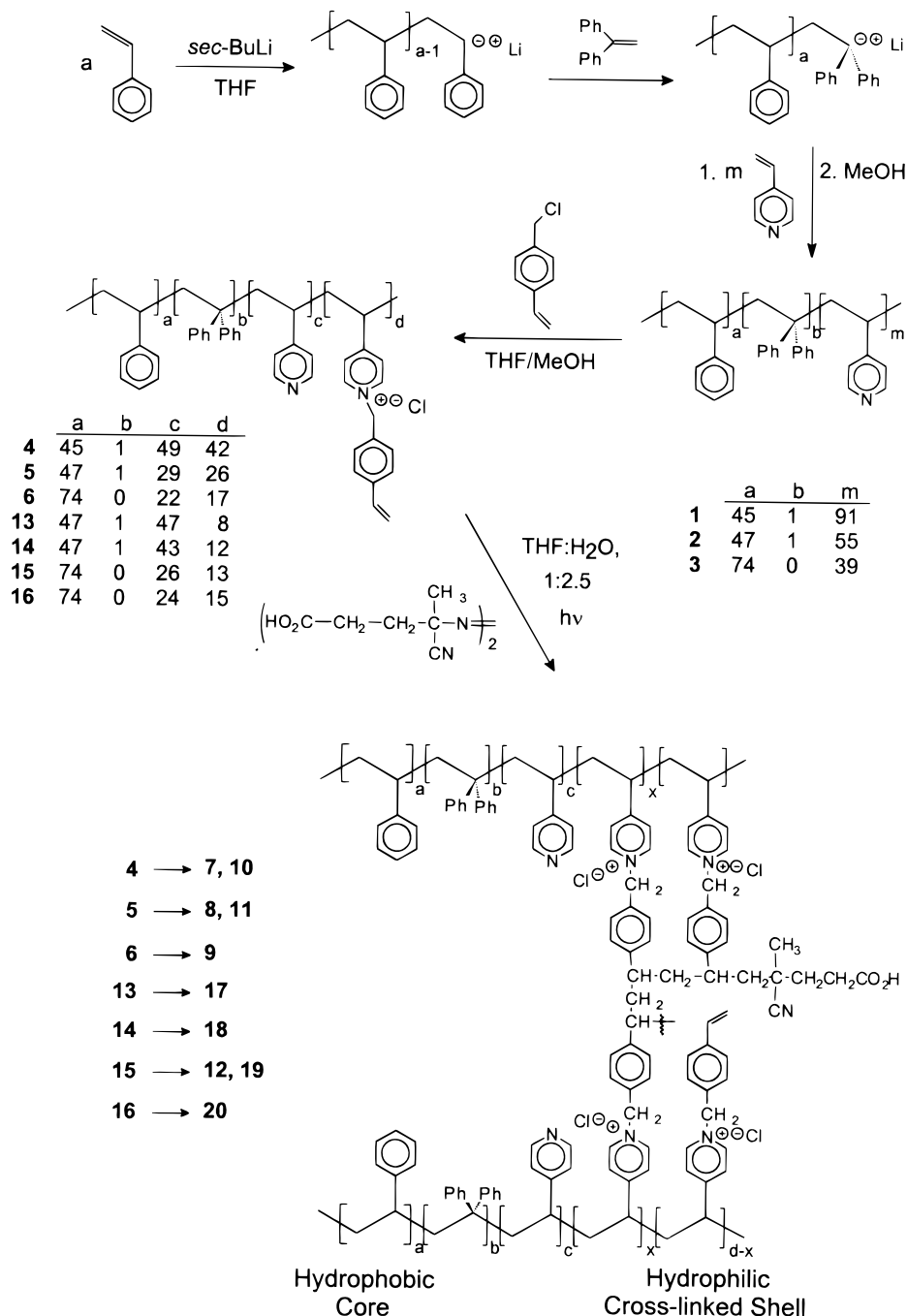
(28) Thurmond, K. B., II; Kowalewski, T.; Wooley, K. L. *J. Am. Chem. Soc.* **1996**, *118*, 7239.

(29) Note: knedel is a Polish word to describe a food of meat surrounded by a dough layer; pronounced k'ned 'l.

(30) A discussion of the comparison of SCK's to dendrimers, hyperbranched polymers, and arborescent polymers (or dendrigrafts) can be found in Wooley, K. L. *Chemistry—A European Journal*, in press.

(31) The formation of radicals from 4,4'-azobis(4-cyanovaleric acid) and subsequent polymerization of the styrenyl groups to effect SCK formation appears to occur by a combination of heat and light. The temperature within the Rayonet photochemical reactor was ~50 °C, at which 4,4'-azobis(4-cyanovaleric acid) has a half-life >100 h. Heating the reaction solution at 50 °C did not result in SCK formation, neither did irradiation at room temperature.

Scheme 1. General Synthetic Approach for the Formation of PS-*b*-PVP **1–3**, Quaternization of a Fraction of the Pyridyl Groups with *p*-(Chloromethyl)styrene To Yield **4–6** and **13–16**, and Polymerization of the Styrenyl Side Groups To Give Cross-Linking of the PVP Domains within the Block Copolymer Micelles, Resulting in the Formation of Shell Cross-Linked Knedels (SCK's) **7–12**, and **17–20**



Differences in the diameters of the SCK's were measured by AFM. As seen in Table 1, with increasing PS percentages, increases in the average SCK diameters are observed, for example, 9, 15, and 23 nm for **7**, **8**, and **9**, respectively. When the content of the block copolymer is 1:2.0 PS:PVP, the smallest SCK is obtained, **7**. An increase in the hydrophobic block length to PS:PVP, 1:1.2, gives an intermediately sized SCK, possessing an intermediate rate of sedimentation or precipitation. Block copolymer **6**, with the greatest polystyrene content, produces the largest micellar aggregates and results in the largest SCK, **9**, which most readily precipitates from solution.

Approximate numbers of polymer chains composing each of the SCK's can be calculated from the AFM diameters, block copolymer molecular weights, and approximate densities,³² giving 12, 79, and 290 as the aggregation numbers for **7**, **8**,

and **9**, respectively. Therefore, the variation in size of the SCK's is due to the differences in the block copolymer aggregation numbers during micelle formation, as well as to the slight variations in molecular weights of the block copolymers.

In Figure 2a, a breadth of particle sizes is apparent for the SCK generated from the 1:2.0 PS:PVP block copolymer. Each of the SCK's shown in Figure 2 was prepared by first allowing the micelles to form over at least a 12 h period of time, followed by addition of the radical initiator and irradiation. It is clear that this is not an optimal method for obtaining uniform particle

(32) The densities were approximated from known densities of PS (1.05 g/mL) and PVP (1.14 g/mL) and from percentages of PS and PVP in each SCK. Densities for **7**, **8**, and **9** were calculated to be 1.11, 1.10, and 1.08 g/mL, respectively.

Table 1. Data for the SCK's

SCK	PS:PVP ratio	polymer molecular weights	percent quaternization	PEO quaternization?	micelle formation time (h)	particle diameter ^a (nm)
Variation in PS:PVP Block Length Ratios						
7	1:2.0	20700	46	NO	17	9 ± 3
8	1:1.2	14600	47	NO	12.5	15 ± 2
9	1.9:1	14400	43	NO	19	23 ± 4
Variation in Micelle Formation Time						
10	1:2.0	20700	46	NO	2.5	7 ± 2
7	1:2.0	20700	46	NO	17	9 ± 3
11	1:1.2	14600	47	NO	2.5	14 ± 2
8	1:1.2	14600	47	NO	12.5	15 ± 2
12	1.9:1	13800	32	NO	1.75	19 ± 4
19	1.9:1	13800	32	NO	12	27 ± 5
Variation in Percent Quaternization						
17	1:1.2	11900	15	NO	13.5	18 ± 3
18	1:1.2	12500	21	NO	19	16 ± 3
8	1:1.2	14600	47	NO	12.5	15 ± 2
19	1.9:1	13800	32	NO	12	27 ± 5
20	1.9:1	14100	38	NO	16	29 ± 2
9	1.9:1	14400	43	NO	19	23 ± 4
Addition of PEO						
24	1:2.0	20700 ^b	46 ^b	YES	18	12 ± 2
7	1:2.0	20700	46	NO	17	9 ± 3
23	1:1.2	14600 ^b	47 ^b	YES	16.5	12 ± 2
8	1:1.2	14600	47	NO	12.5	15 ± 2
22	1.9:1	13800 ^b	32 ^b	YES	18	22 ± 4
19	1.9:1	13800	32	NO	12	27 ± 5

^a Number average particle heights from measurement of 200–300 particles by tapping mode AFM of SCK's adsorbed onto mica. Uncertainties are calculated as standard deviations of average particle sizes. ^b The molecular weights and quaternization percentages for **22**–**24** are prior to PEO quaternization.

sizes, so the effect of micelle formation time upon the particle size and size distribution was studied.

Micelle Formation Time. The particle size distribution plots for **10**, **11**, and **12** prepared with ~2 h micelle formation time from 1:2.0, 1:1.2, and 1.9:1 PS:PVP are shown in Figure 3, with the average SCK sizes being 7, 14, and 19 nm, respectively. As the time allowed for micelle formation is increased, secondary micelles of increased sizes are formed, with both primary and secondary micelles being observed (Figure 4). The increased sizes for the SCK's can result from a combination of increased aggregation numbers of polymer chains and coalescence of micelles. Coalescence of the positively charged shells seems unfavorable; however, the presence of the relatively large hydrophobic styrenyl unit used for quaternization along the PVP backbone may decrease the electrostatic repulsions and allow for surface tension effects and van der Waals interactions between the surfaces to dominate. Due to the apparent bimodal size distributions with discrete size increases, coalescence appears to be the predominant growth mechanism.

The 1:2.0 PS:PVP system gave the largest percentage increase in diameter (100%) between the primary and secondary micelles, which corresponds to an ~8-fold volume increase. In this case, the relatively short hydrophobic PS block length may form a smaller and less stable PS core. For the 1.9:1 PS:PVP system, significant populations of primary and secondary micelles were also observed, with an ~50% diameter increase, corresponding to an ~3-fold volume increase. The 1:1.2 PS:PVP system formed polymer micelles that did not significantly change in size over time. For the remainder of the studies of composition vs SCK sizes, longer micelle formation times were used to evaluate both the primary and secondary micelle sizes and to provide comparison of the propensity for aggregation between differing systems.

Quaternization Effects. To broaden the types of SCK's that can be prepared from a single block copolymer, variation in

the quaternization percentages and quaternization species were studied. The large number of pyridyl groups along each of the block copolymers provides numerous sites for the introduction of multiple species to alter the physical and chemical properties of the SCK's. Initially, the effect of the percent of pyridyl salts present in the block copolymers, **4**–**6** and **13**–**16** upon their micellization and SCK formation was studied. Further alteration of the SCK was made by the incorporation of PEO through quaternization of the polymer backbone with monofunctional PEO prior to cross-linking.

Differences in the quaternization percentages of polymer **2** were investigated with the formation of block copolymers **13**, **14**, and **5**, which gave SCK's **17**, **18**, and **8**, containing respectively 15, 21, and 47% of the pyridyl groups quaternized. During the formation of **17**, a precipitate formed, while **18** was soluble during irradiation, but then began to form precipitate after ~10 days. These observations, along with the fact that **8** was soluble for a month, indicate that increasing the quaternization percentage leads to increasing water solubility for the SCK's. Further substantiation of this conclusion is seen in comparison of **9** with **19** and **20**. The SCK's **19** and **20** had similar solubility characteristics, in which they both were less soluble than **9**, and both seemed to begin to precipitate during the SCK formation with even more material settling out of solution over time (2–3 months). This demonstrated that lower amounts of charged sites along the PVP chain decreases the hydrophilicity and electrostatic effects, thereby decreasing the water solubility. It should be noted that increasing amounts of quaternization by *p*-(chloromethyl)styrene also gives increasing numbers of cross-linkable groups, which could lead to higher cross-link densities and further modification of the properties (e.g. shell penetrability, rigidity, stability, etc.) of the SCK's.

Larger average particle diameters were observed by AFM with lower quaternization percentages. SCK **9** had an average diameter of 23 ± 4 nm, but slight changes in the quaternization percentage resulted in only slight changes in the diameters: 27 ± 5 and 29 ± 2 nm for SCK's **19** and **20**, respectively. These values are within the measured margin of error, thus seemingly indicating no real change in the particle diameter. However, comparison of the particle size distribution analyses indicates that the SCK's are quite different. As shown in Figure 5 and Figure 4c, the average SCK diameter for **9** is 23 nm and **19** is 17% larger with the highest number of SCK's having a diameter of 27 nm. These SCK samples were prepared with long equilibration times, so the aggregation behavior can be discerned from comparison of the primary and secondary sizes of each, in which an increase in diameter of 25% corresponds to an approximate doubling of the volume. The increase in size upon growth from the primary micelles to the secondary micelles for **9** is ~30%, indicating combination of two micelles during coalescence to give the thermodynamically favored micelles. In contrast, the diameter of the polymer micelles in the formation of **19** increases by 45% from the primary micelles of 19 nm to the secondary structures of 27 nm diameter. This increase corresponds to coalescence of *ca.* three primary micelles and suggests that the block copolymer used for the construction of **19** has a stronger drive to aggregate than that used for the preparation of **9**. In addition, the size distribution analysis plot of **19** contains a tail extending toward larger particles, resulting from even higher aggregation. SCK **19** was prepared from **15**, with 32% quaternization of the pyridyl groups, and **9** was prepared from **6** with 43% quaternization. Therefore, the lower hydrophilicity of **15** results in a higher propensity for aggregation and the production of larger SCK's, in comparison to **6**.

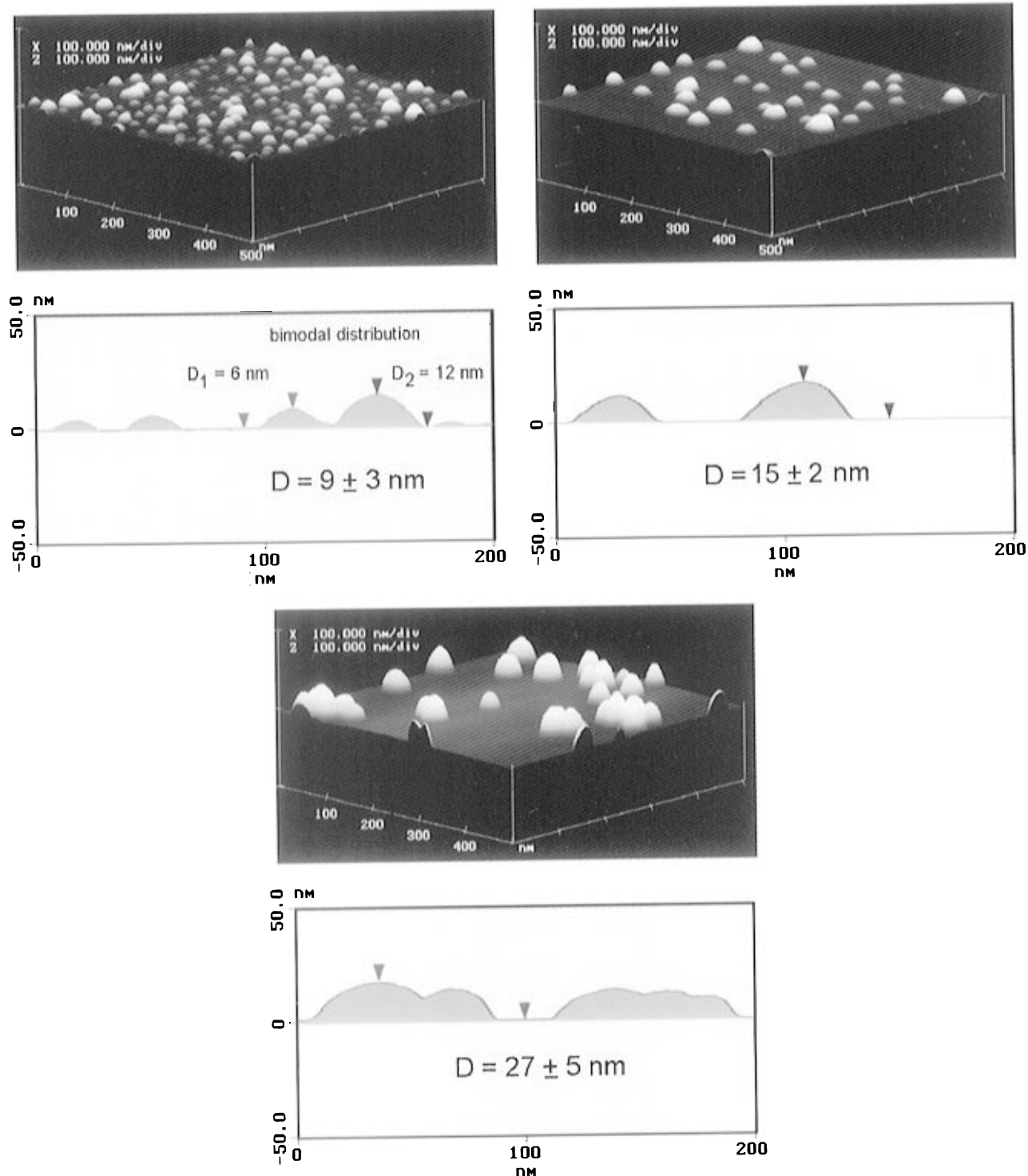


Figure 2. Tapping mode AFM images and height profiles of SCK's adsorbed on freshly cleaved mica (a, top left) **7**, (b, top right) **8**, (c, bottom) **9**; prepared from 1:2.0, 1:1.2, and 1.9:1 PS:PVP block copolymers, respectively, each with ~45% of the pyridyl nitrogen atoms quaternized by *p*-(chloromethyl)styrene. The lateral sizes of the particles are distorted due to the finite size of the AFM tip; therefore, the particle diameters were measured from the particle heights. Profiles of individual particles are consistent with spheres of diameters corresponding to the heights of the images "convoluted" with a tip of ~15 nm radius (typical radius of silicon tips used throughout this study).

Another method to alter the properties of the SCK's involved incorporation of poly(ethylene oxide) (PEO) into the hydrophilic shell. PEO has been shown to increase the blood circulation time and cause body distribution differences for polymer micelles,¹ which could also prove to be important for potential applications of SCK's. Therefore, **15** was treated with mono-methyl ether bromo(polyethylene oxide) ($M_w = 1950$), **21**, and the micellar aggregate of the resulting block-graft copolymer was polymerized *in situ*. The PEO-functionalized SCK's displayed improved water solubility, in comparison to the SCK's

lacking PEO. For example, upon completion of cross-linking, the aqueous solution of **22** appeared to be significantly less turbid than for the corresponding nonfunctionalized SCK **19**. The same approach was used in the formation of **23**, from block copolymer **5** and **21**. In this case, **23** remained in solution for up to 3 months while the non-PEO 1:1.2 PS:PVP SCK, **8**, began to precipitate after 1 month. Importantly, the incorporation of PEO facilitated the resolubilization of freeze-dried SCK samples, in contrast to SCK's with no PEO, for which dried samples could not be resolubilized.

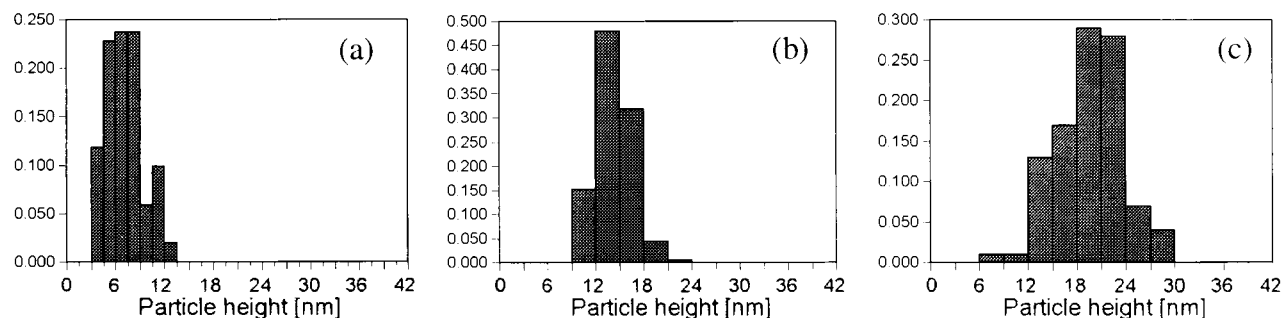


Figure 3. Histograms of fractions of particles *vs* particle heights (nm) to illustrate the size distributions of the SCK's (a) **10**, (b) **11**, (c) **12**, each prepared with short (~2 h) micelle formation times prior to cross-linking.

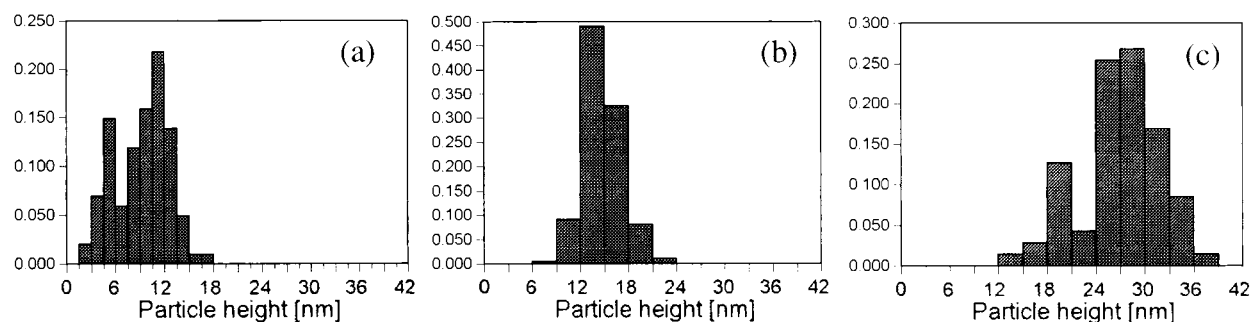


Figure 4. Histograms of fractions of particles *vs* particle heights (nm) to illustrate the size distributions of the SCK's (a) **7**, (b) **8**, (c) **19**, each prepared with long (>12 h) micelle formation times prior to cross-linking.

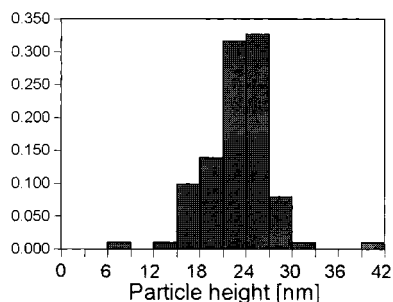


Figure 5. Histograms of fractions of particles *vs* particle heights (nm) to illustrate the size distributions of the SCK **9**, from 1.9:1 PS:PVP, 43% quaternization, and prepared with long (19 h) micelle formation time prior to cross-linking.

The PEO increased the hydrophilic nature of the block copolymers to aid in their water solubility, which also decreased the aggregation numbers of the micelles, to yield SCK's of smaller diameters. Comparisons of **8** with **23** and **19** with **22** show slight decreases in size upon the addition of PEO. In addition, the size distributions narrowed with the addition of the PEO.

Characterization. The ^1H NMR spectra of the quaternized block copolymers displayed resonances for each of the different protons within the structures. Qualitatively, the intensities of the resonances agreed with the compositions of the block copolymers. However, due to incomplete solvation of the entire amphiphilic block copolymers, the integration values of the protons did not allow for accurate calculation of the amount of quaternization. Therefore, quaternization values were obtained by elemental analysis.

Characterization of the SCK's by solution state NMR was complicated by further solubility problems. Although the SCK's appear to be dissolved in water, existing as transparent light yellow-colored solutions, no resonances are observable in the solution state ^1H NMR spectra of SCK's in D_2O . Once filtered and diluted, the SCK's remain suspended within an aqueous solution, but it was not possible to resolubilize the SCK's after

removal of the water, even using mixtures of solvents and sonication. Therefore, the SCK's behave as cross-linked materials. An exception to this behavior was found with the incorporation of PEO. The PEO-functionalized SCK's could be freeze-dried and resuspended directly into water.

An interesting finding was that addition of $\text{THF-}d_8$ to a D_2O solution of SCK results in observable styrenyl aromatic and aliphatic ^1H resonances.²⁸ This demonstrates that even though the SCK shell is several nanometers thick and cross-linked, the THF can migrate into the core of the structure and solvate the PS chains. When a 10 mL solution of PEO-functionalized SCK **23** was freeze-dried, the resulting film was soluble in a 2:1 $\text{D}_2\text{O}/\text{THF-}d_8$, and gave an ^1H NMR spectrum that showed resonances indicative of the protons of the PEO chains, as well as some aliphatic protons and the aromatic protons of the non-cross-linked PS core. The shell penetrability was also noted by the inclusion of pyrene which gave excitation spectra corresponding to the hydrophobic core environment of the SCK; there was no evidence of a cmc upon dilution of SCK solutions to 10^{-11} M (concentration based upon polymer chains).

Due to the insolubility of the cross-linked shells, solid state NMR proved invaluable in the overall SCK characterization. Solid state ^{13}C NMR spectra displayed broad resonances in the frequency ranges expected for the SCK composition. Infrared spectroscopy was also useful, in the confirmation of the composition of the entire SCK.

Static sessile drop contact angle measurements³³ of H_2O on the surfaces of the SCK's and homopolymer samples of the block copolymer components were performed to determine the surface characteristics and compositions of the SCK's. A contact angle of 63° was measured for H_2O upon PVP (MW = 50 000), while *p*-(chloromethyl)styrene-quaternized PVP (25–60%) gave values of 53 – 56° , and the contact angle of H_2O on PS (MW = 45 000) was found to be 92° . Contact angle measurements for SCK's **7**, **8**, and **9** gave values of 46° , 49° , and 40° ($\pm 4^\circ$). Comparison of the SCK contact angles with

Table 2. T_g 's ($^{\circ}\text{C}$) of the PS and PVP blocks of **4**–**6**. Obtained from DSC Scans with Heating Rates of $10^{\circ}\text{C}/\text{min}$ over the Temperature Range from 50 to 220°C .

DSC heating scan no.	4		5		6		13	
	$(T_g)_{\text{PS}}$	$(T_g)_{\text{PVP}}$	$(T_g)_{\text{PS}}$	$(T_g)_{\text{PVP}}$	$(T_g)_{\text{PS}}$	$(T_g)_{\text{PVP}}$	$(T_g)_{\text{PS}}$	$(T_g)_{\text{PVP}}$
second	80	183	93			<i>a</i>	98	148
third	83	187	94	193	97	<i>b</i>	103	158
fourth	82	191	92	197	96	<i>b</i>	102	154
fifth	78	199	92	200	96	<i>b</i>	100	157

^a A broad endotherm was observed from 120 to 190°C . ^b A broad endotherm was observed from 120 to 220°C .

those of PS, PVP, and quaternized PVP indicated that quaternized PVP was indeed composing the shell and that at least some of the quaternized sites were near the SCK surface, resulting in a positively charged and hydrophilic nanosphere. The hydrophilic nature of the PEO-functionalized SCK's gave even lower contact angle values; however, the measurements were complicated by dissolution of these SCK's into the water.

Differential scanning calorimetry (DSC) and thermogravimetric analysis (TGA) were used for the thermal analysis of the quaternized block copolymers and the SCK's. For the block copolymers, glass transition temperatures (T_g) were observed for both the PS and the PVP domains (Table 2). The PS T_g 's depended upon the molecular weight of the PS block, the ratio of the PS:PVP block lengths, and the percent quaternization of the PVP. As expected, the T_g increased with increasing molecular weight, in which **6** exhibits a higher T_g than **4** and **5**. Interestingly, **4** displays a lower T_g than **5**, even though their molecular weights are *ca.* equal (M_w 's of 4700 and 4900, respectively), which suggests that smaller PS domains for **4** may result in lower T_g 's. Comparison of the T_g 's for **4** and **13** indicates that phase separation differs with extent of PVP quaternization, resulting in differing T_g 's for the PS phase. In addition, the T_g of the PVP phase is lower with lower percentages of quaternization. Both **4** and **5** have significant PVP content and similar percentages of quaternization, resulting in comparable T_g 's for the PVP phase, which are higher than that of **13**. In contrast, **6** exhibits only a broad endotherm from ~ 120 to 200°C . Increases in the T_g 's for the PVP blocks were observed over successive runs, probably due to the occurrence of cross-linking at elevated temperatures.³⁴

Each of the SCK's gave similar results by DSC, in which no explicit transitions were evident for the PS or for the PVP domains, but a broad endotherm was detected in each run ranging from ~ 100 to 180°C , followed by a broad exotherm above 200°C . The exotherm corresponded to decomposition onset exhibited in the TGA scans. The TGA runs typically showed onset of decomposition at ~ 180 – 200°C , with 2–10% mass loss, followed by 40–70% mass loss from 250 to 425°C .

Conclusions

Amphiphilic core-shell nanometer sized spheres have been prepared as single shell cross-linked macromolecular assemblies, by the organization of amphiphilic block copolymers into micellar assemblies followed by stabilization of the structures through cross-linking of the outer shell of the spherical polymer micelles. Due to the method of production, the sizes and compositions are accurately controlled by variation in the hydrophobic/hydrophilic block length ratios, the nature of the hydrophilic block (e.g. the properties of the quaternizing species and the extent of quaternization for the PVP material), and the

time allowed for micelle formation. Differences in the relative block lengths were found to have the most dramatic effect upon the aggregation numbers of the polymer micelles and, therefore, upon the diameters of the resulting SCK's. In addition, the core diameter and shell thickness are also affected by the relative block molecular weights of the block copolymers. The reactivity of the pyridyl units toward quaternization was used both to attach functionality and to alter the properties of the SCK's. Variation in the extent of incorporation of cross-linkable functionalities leads to differences in the cross-link density of the SCK shell; however, under all cases studied, the shell remained penetrable.

Further modification of the chemical compositions and characterization of the structures of the SCK's are in progress. We are currently taking advantage of the unique SCK core environment for encapsulation and also the shell reactivity for surface interactions to investigate the ability for SCK's to serve as mimics of biological delivery agents. Important characteristics of the SCK's resemble those of polymer micelles, including their core-shell morphology, controllable nanometer-size range, narrow size distribution, water solubility, and ease of synthesis. However, the significant improvement is that the SCK's are stable structures, which are not destroyed by dilution (may be important for *in vivo* applications), and they resist deformation under shear forces. The SCK's are expected to be superior materials for applications targeted for non-cross-linked polymer micelles, as well as those for liposomes, and dendrimers, such as gene therapy, drug delivery, coatings, etc., in which the surface can be employed for binding and recognition while the core composition can be tailored for encapsulation and release.

Experimental Section

Measurements. IR spectra were obtained on a Mattson *polaris* spectrometer as KBr pellets. ^1H NMR spectra were recorded as solutions on either a Varian Unity 300 MHz spectrometer or a Varian Gemini 300 MHz spectrometer with the solvent proton signal as standard. ^{13}C NMR spectra were recorded at 75.4 MHz as solutions on either a Varian Unity 300 spectrometer or on a Varian Gemini 300 spectrometer with the solvent carbon signal as standard. Cross-polarization magic-angle spinning ^{13}C NMR spectra were obtained at room temperature on a DNP CPMAS spectrometer³⁵ built around a horizontal 6-in. bore Oxford superconducting solenoid operating at a proton Larmor frequency of 60 MHz, 15.1 MHz for carbons. Lyophilized samples (200–300 mg) were spun at 1859 Hz, and experiments began with 1-ms matched spin-lock cross-polarization transfers from protons at 50 kHz followed by proton decoupling at 90 kHz. The sequence repetition time for all experiments was 1 s.

Gel permeation chromatography (GPC) was conducted on a Hewlett-Packard series 1050 HPLC with a Hewlett-Packard 1047A refractive index detector: data analysis was done by Viscotek (Houston, TX) Trisec GPC Software, v. 2.70. Two $5\text{-}\mu\text{m}$ Polymer Laboratories PL gel columns ($300 \times 7.7\text{ mm}$) connected in series, in order of increasing pore size (500 \AA , mixed bed E), were used with THF distilled from CaH_2 as solvent. Glass transition temperatures were measured by differential scanning calorimetry on a Perkin-Elmer DSC-4 differential scanning calorimeter. Heating rates were $10^{\circ}\text{C}/\text{min}$, and T_g was taken as the midpoint of the inflection tangent upon the third heating scan. The Perkin-Elmer instrument was upgraded with Instrument Specialists, Inc. (Antioch, IL) temperature program interface-PE, and data were acquired and analyzed using TA-PC software version v. 2.11 (Instrument Specialists, Inc.). Irradiation was carried out in a Rayonet photochemical reactor containing Hg lamps. Contact angles were measured as static contact angles with the sessile drop technique³³ using a Tanteq CAM-micro contact angle meter and the half-angle measuring method. The samples were prepared by solution casting of the materials

(34) Hale, A.; Macosko, C. W.; Bair, H. E. *Macromolecules* **1991**, *24* (9), 2610.

(35) Afeworki, M.; McKay, R. A.; Schaefer, J. *Macromolecules* **1992**, *25*, 4084.

onto a microscope slide to produce films of ~ 0.5 mm thickness. Contact angles of water drops (4 μL) on the films were measured 30 s after drop application, and an average of five measurements is given.

Samples for AFM imaging were prepared by placing a 2 μL drop of suspension of SCK's (typical concentration about 10 μM) on freshly cleaved mica (Ruby clear mica, New York Mica Co.) and allowing it to dry freely. Such prepared samples were imaged immediately after deposition as well as after several days without noticeable changes in appearance and average dimensions. AFM imaging was performed with the aid of Nanoscope III-M system (Digital Instruments, Santa Barbara, CA) operating in tapping mode and equipped with a J-type vertical engage piezoelectric scanner. Standard etched silicon probes (1 = 120 μm , spring constant ~ 50 N/m, resonance frequency ~ 300 kHz) were used throughout the study. Typical scan frequencies were between 1.5 and 5 Hz, depending on scan fields, which varied from 4 $\mu\text{m} \times 4 \mu\text{m}$ to 500 nm \times 500 nm. In tapping mode imaging, the cantilever is oscillated above the surface at a frequency close to its resonance frequency and touches it intermittently at the peak of each oscillation cycle. The decrease of cantilever oscillation amplitude due to intermittent contacts is used as a control signal for a feedback loop for tracking the surface topography. Throughout this study, tapping mode imaging was carried-out with cantilever oscillation amplitudes of about 10 nm. The typical value of a ratio of "tapping" amplitude to "free" cantilever oscillation amplitude was equal to 0.95. The SCK diameters were taken as the heights of the SCK's, which were measured with the aid of bearing analysis procedure, using Nanoscope III software package. Distributions of heights of the SCK's were obtained from individual measurements performed on 100–200 particles.

Materials. Argon (99.9995%) was used for all manipulations and storage of materials. Styrene (Aldrich) and 4-vinylpyridine (Aldrich) were distilled from CaH_2 three times each and stored in the freezer. Prior to polymerization, styrene was transferred via syringe followed by addition of dibutylmagnesium (Aldrich) until a pale yellow color was evident. The mixture was then allowed to stir for 30 min. The solution was degassed three times and vacuum distilled. Also prior to polymerization, 4-vinylpyridine was added to CaH_2 and the mixture allowed to stir for 1–2 h. The solution was degassed three times and distilled. 1,1-Diphenylethylene, prepared according to the literature³⁶ procedure, was degassed three times, *sec*-BuLi was then added until a deep cherry red color was obtained. The solution was allowed to stir for 30 min, was degassed an additional three times, and was vacuum-distilled. Dry THF (distilled from purple potassium/benzophenone ketyl) was transferred via cannula to a flask containing Na/benzophenone, degassed three times, and vacuum-distilled directly into the reaction flask. *sec*-Butyllithium (Acros, 1.3 M in cyclohexane/hexane), *p*-(chloromethyl)styrene (Aldrich, 97%), 4,4'-azobis(4-cyanovaleric acid) (Acros 97%), and water (Sigma-Aldrich HPLC Grade) were used as received. The concentration of the *sec*-butyllithium initiator was determined by titration with 2,5-dimethoxybenzyl alcohol in dry, freshly distilled THF.

General Procedure of the Anionic Polymerization of 1–3. All purification of reagents and solvents (as described above) and polymerizations were done on a double manifold connected to a high vacuum line (10^{-6} mmHg) and argon (99.9995%). Styrene in THF at -75 $^\circ\text{C}$ under Ar was initiated with the addition of *sec*-butyllithium via syringe. In the polymerizations of **1** and **2** the living polystyrene was capped with 1 equiv of 1,1-diphenylethylene after ~ 20 min of polymerization. In all cases, a small portion of the living PS was removed and quenched in degassed methanol to allow for the determination of the PS block molecular weight by GPC. 4-Vinylpyridine was transferred via cannula into the polymerization mixture and allowed to stir for 1.5 h. The living block copolymer was then quenched with degassed methanol. Removal of *ca.* half of the THF was performed *in vacuo*, followed by precipitation of the polymer into at least a 10-fold excess of hexane. Subsequent filtering and drying yielded a white powder. Because approximate amounts of the monomers were used, the percent yields of polymers were not calculated. The PS M_n , M_w , and M_w/M_n values were determined from GPC based upon calibration with PS standards. The PVP and PS-*b*-

PVP M_n values were determined by comparison of the unique aromatic proton resonances of pyridyl (8.1–8.5 ppm) and styrenyl (6.2–6.7 ppm) repeat units.

Polystyrene-*b*-poly(vinylpyridine) (1). A total of 28.9 g was isolated. The PS used in this block copolymer had a $M_w = 4700$ with a polydispersity of 1.17 (M_w/M_n). The molecular weight of the PVP block was 9600, which gives a total molecular weight of 14 300 for the block copolymer.

Polystyrene-*b*-poly(vinylpyridine) (2). A total of 42.25 g was isolated. The PS used in this block copolymer had a $M_w = 4900$ with a polydispersity of 1.14 (M_w/M_n). The molecular weight of the PVP block was 5800, which gives a total molecular weight of 10 700 for the block copolymer.

Polystyrene-*b*-poly(vinylpyridine) (3). A total of 19.46 g was isolated. The PS used in this block copolymer had a $M_w = 7700$ with a polydispersity of 1.10 (M_w/M_n). The molecular weight of the PVP block was 4100, which gives a total molecular weight of 11 800 for the block copolymer.

General Procedure for Quaternization of Polystyrene-*b*-poly(vinylpyridine) with *p*-(Chloromethyl)styrene. These reactions were carried out on quantities varying from 2 to 6 g. To a flame-dried 100 mL round bottom flask was added PS-*b*-PVP (1 equiv) and THF (20–25 mL). After ~ 2 h of stirring under a N_2 flow, *p*-(chloromethyl)styrene (15–100 equiv based upon polymer chains) was added. A pale yellow color was almost immediately evident. The flask was covered with aluminum foil and stirred for 16–17 h, and then MeOH (20–25 mL) was added. A more intense yellow became evident over the next few hours. After 2.5 days, MeOH (7 mL) was added and an additional portion of MeOH (7 mL) was added 12 h later. Samples were taken periodically and precipitated into hexane, filtered, and dried. If ^1H NMR indicated incomplete quaternization (presence of sharp vinyl peaks), then an additional amount of MeOH (~ 7 mL) was added. This process was repeated every 12 h. Over this time, the reaction mixture color changed to a blue/green. The total stirring time of the reaction ranged from 100 to 190 h. The reaction mixture was then precipitated into hexane and allowed to settle for 4–8 h. The hexane was decanted off, and the green solid was dried *in vacuo* for 1–2 days: IR (KBr) 3100–2960, 2930–2800, 1950, 1870, 1810, 1640, 1600, 1560, 1490, 1450, 1420, 1380–1320, 1230, 1160, 1080, 1040, 1010, 910, 840, 770, 710 cm^{-1} ; ^1H NMR ($\text{CD}_3\text{OD}:\text{CDCl}_3$, 2:1) δ 1.1–2.0 (br m, CH_2 and CH of backbone), 5.1–5.2 (br d, $J = 10$ Hz, (*trans* $\text{CH}=\text{CHPh}$)_{Styrene}), 5.3–5.8 (br m, (*cis* $\text{CH}=\text{CHPh}$)_{Styrene} and $\text{PyrN}^+\text{CH}_2\text{Styrene}$), 6.2–6.7 (br m, (2 ortho ArH)_{PS}, (2 ArH)_{PVP}, *gem* $\text{CH}_2=\text{CHPh}$)_{Styrene}), 6.7–7.0 (br m, (2 meta ArH and para ArH)_{PS}), 7.1–7.5 (br m, (2 ArH)_{quat. PVP} and (4 ArH)_{Styrene}), 7.8–8.2 (br m, (2 ArH)_{PVP}), 8.2–8.8 (br m, (2 ArH)_{quat. PVP}) ppm.

Polystyrene-*b*-poly(vinylpyridine)-*N*-(chloromethyl)styrene (4). This was prepared from PS-*b*-PVP **1** (5.30 g, 0.371 mmol) and *p*-(chloromethyl)styrene (5.29 g, 35 mmol) with total quaternization time being 170 h to give **4** as a green solid. The fraction of pyridyl groups that were quaternized was found to be 46%, based upon the elemental analysis data for the percentages of Cl and N: yield 7.64 g (99%); (T_g)_{PS} = 83 $^\circ\text{C}$, (T_g)_{PVP} = 187 $^\circ\text{C}$. Anal. Calcd for $\text{C}_{1375}\text{H}_{1375}\text{N}_9\text{Cl}_{42}$ (20 700): C, 79.92; H, 6.71; N, 6.17; Cl, 7.21. Found: C, 72.27; H, 6.74; N, 5.82; Cl, 6.82.

Polystyrene-*b*-poly(vinylpyridine)-*N*-(chloromethyl)styrene (5). This was prepared from PS-*b*-PVP **2** (4.65 g, 0.435 mmol) and *p*-(chloromethyl)styrene (3.96 g, 26 mmol) with total quaternization time being 120 h to give **5** as a green solid. The fraction of pyridyl groups that were quaternized was 47%, based upon the elemental analysis data for the percentages of Cl to N: yield 6.20 g (98%); (T_g)_{PS} = 94 $^\circ\text{C}$, (T_g)_{PVP} = 193 $^\circ\text{C}$. Anal. Calcd for $\text{C}_{995}\text{H}_{995}\text{N}_{55}\text{Cl}_{26}$ (14 600): C, 81.60; H, 6.85; N, 5.26; Cl, 6.29. Found: C, 77.35; H, 7.12; N, 4.92; Cl, 5.84.

Polystyrene-*b*-poly(vinylpyridine)-*N*-(chloromethyl)styrene (6). This was prepared from PS-*b*-PVP **3** (2.94 g, 0.249 mmol) and *p*-(chloromethyl)styrene (1.90 g, 12.4 mmol) with total quaternization time being 185 h to give **6** as a green solid. The fraction of pyridyl groups that were quaternized was 43%, based upon the elemental analysis data for the percentages of Cl to N: yield 3.27 g (91%); (T_g)_{PS} = 97 $^\circ\text{C}$, (T_g)_{PVP} = not observed. Anal. Calcd for $\text{C}_{1018}\text{H}_{1018}\text{N}_{59}\text{Cl}_{17}$

(36) Allen, C. F. H.; Converse, S. *Organic Syntheses*; Wiley: New York, 1941; Collect. Vol. I, p 226.

(14 400): C, 84.90; H, 7.12; N, 3.79; Cl, 4.18. Found: C, 82.99; H, 7.53; N, 3.54; Cl, 3.85.

Polystyrene-*b*-poly(vinylpyridine)-*N*-(chloromethyl)styrene (13). This was prepared from PS-*b*-PVP **2** (3.08 g, 0.288 mmol) and *p*-(chloromethyl)styrene (0.66 g, 4.35 mmol) with total quaternization time being 117 h to give **13** as a green solid. The fraction of pyridyl groups that were quaternized was 15%, based upon the elemental analysis data for the percentages of Cl to N: yield 3.25 g (95%); (T_g)_{PS} = 103 °C, (T_g)_{PVP} = 158 °C. Anal. Calcd for C₈₃₃H₈₃₃N₅₅Cl₈ (11 900): C, 84.09; H, 7.06; N, 6.47; Cl, 2.38. Found: C, 81.99; H, 6.99; N, 6.21; Cl, 2.37.

Polystyrene-*b*-poly(vinylpyridine)-*N*-(chloromethyl)styrene (14). This was prepared from PS-*b*-PVP **2** (3.06 g, 0.286 mmol) and *p*-(chloromethyl)styrene (1.20 g, 7.85 mmol) with total quaternization time being 117 h to give **14** as a green solid. The fraction of pyridyl groups that were quaternized was 21%, based upon the elemental analysis data for the percentages of Cl to N: yield 3.29 g (92%); (T_g)_{PS} = 98 °C, (T_g)_{PVP} = not observed. Anal. Calcd for C₈₆₉H₈₆₉N₅₅Cl₁₂ (12500): C, 86.38; H, 7.25; N, 6.38; Cl, 3.52. Found: C, 81.15; H, 7.45; N, 6.01; Cl, 3.24.

Polystyrene-*b*-poly(vinylpyridine)-*N*-(chloromethyl)styrene (15). This was prepared from PS-*b*-PVP **3** (4.54 g, 0.385 mmol) and *p*-(chloromethyl)styrene (2.32 g, 15.2 mmol) with total quaternization time being 132 h to give **15** as a green solid. The fraction of pyridyl groups that were quaternized was 32%, based upon the elemental analysis data for the percentages of Cl to N: yield 5.29 g (99%); (T_g)_{PS} = 101 °C, (T_g)_{PVP} = 176 °C. Anal. Calcd for C₉₈₂H₉₈₂N₃₉Cl₁₃ (13800): C, 85.52; H, 7.18; N, 3.96; Cl, 3.34. Found: C, 83.60; H, 7.07; N, 3.97; Cl, 3.25.

Polystyrene-*b*-poly(vinylpyridine)-*N*-(chloromethyl)styrene (16). This was prepared from PS-*b*-PVP **3** (2.86 g, 0.242 mmol) and *p*-(chloromethyl)styrene (1.40 g, 9.15 mmol) with total quaternization time being 185 h to give **16** as a green solid. The fraction of pyridyl groups that were quaternized was 38%, based upon the elemental analysis data for the percentages of Cl to N: yield 3.30 g (97%); (T_g)_{PS} = 101 °C, (T_g)_{PVP} = 175 °C. Anal. Calcd for C₁₀₀₀H₁₀₀₀N₃₉Cl₁₅ (14 100): C, 85.20; H, 7.15; N, 3.88; Cl, 3.77. Found: C, 83.39; H, 7.27; N, 3.60; Cl, 3.50.

General Procedure for Micellization and Cross-Linking of Polystyrene-*b*-poly(vinylpyridine)-*N*-(chloromethyl)styrene To Form SCK's. To a 250 mL quartz reaction vessel was added polystyrene-*b*-poly(vinylpyridine)-*N*-(chloromethyl)styrene and appropriate volumes of THF and then H₂O to give a solution concentration from 5×10^{-5} to 9×10^{-5} M and a THF:H₂O ratio of approximately 1:2.5. A septum was placed in the flask, and the reaction mixture was stirred under a N₂ flow for 1.75–19 h, depending upon the experiment. The initiator 4,4'-azobis(4-cyanovaleric acid) was then added and allowed to stir for up to 2 h. Irradiation was then performed on the open flask for 24 h within a Rayonet photochemical reactor, which resulted in a decrease in volume due to loss of ~50% of the THF from the heat generated by the lamp during irradiation. All samples were filtered through a 0.45 μm PTFE filter, and AFM was performed. Spectroscopic characterization for each of the SCK's included the following data: IR (KBr) 3530–3100, 3060, 3030, 3000, 2940–2820, 1740–1680, 1650, 1600, 1560, 1480, 1470, 1450–1370, 1280, 1240–1170, 1100–1040, 780, 710 cm⁻¹; solution state ¹H NMR (D₂O:THF-*d*₈, 3:1) δ 1–2.8 (aliphatic protons of polymer backbone and initiator), 6.3–7.5 (aromatic protons of PS) ppm; solid state ¹³C NMR δ 10–50 (PS and PVP aliphatic backbone, initiator methyl and methylene carbons), 50–75 (benzylic methylenes of *p*-(chloromethyl)styrene-quaternized PVP and initiator methine), 110–150 (PS and PVP aromatic carbons), 150–165 (initiator carboxylic acid carbonyl) ppm.

SCK 7. This was prepared from **4** (0.35 g, 0.017 mmol) in THF (70 mL), and H₂O (170 mL) and allowed to stir for 16 h. 4,4'-Azobis(4-cyanovaleric acid) (0.17 g, 0.59 mmol) was added (63 mol % based on available styrenyl groups), and the reaction mixture was allowed to stir for 1 h prior to irradiation for 24 h. During irradiation, the solution changed color from very light green to bright yellow. An average diameter of 9.0 ± 3.0 nm was obtained from AFM.

SCK 8. This was prepared from **5** (0.21 g, 0.014 mmol) in THF (70 mL), and H₂O (180 mL) and allowed to stir for 12 h. 4,4'-Azobis(4-cyanovaleric acid) (0.08 g, 0.29 mmol) was added (63 mol % based

on available styrenyl groups), and the reaction mixture was allowed to stir for 0.5 h prior to irradiation for 24 h. During irradiation, the solution changed color from very light green to bright yellow. An average diameter of 15 ± 2 nm was obtained from AFM.

SCK 9. This was prepared from **6** (0.23 g, 0.016 mmol) in THF (60 mL), and H₂O (150 mL) and allowed to stir for 17.75 h. 4,4'-Azobis(4-cyanovaleric acid) (0.05 g, 0.18 mmol) was added (61 mol % based on available styrenyl groups), and the reaction mixture was allowed to stir for 1.25 h prior to irradiation for 24 h. During irradiation, the solution changed color from very light green to yellow with an oil-like precipitate forming on the sides of the flask. An average diameter of 23 ± 4 nm was obtained from AFM.

SCK 10. This was prepared from **4** (0.24 g, 0.012 mmol) in THF (70 mL), and H₂O (180 mL) and allowed to stir for 2 h. 4,4'-Azobis(4-cyanovaleric acid) (0.11 g, 0.40 mmol) was added (64 mol % based on available styrenyl groups), and the reaction mixture was allowed to stir for 0.5 h prior to irradiation for 24 h. During irradiation, the solution changed color from very light green to a light yellow. An average diameter of 7 ± 2 nm was obtained from AFM.

SCK 11. This was prepared from **5** (0.21 g, 0.014 mmol) in THF (70 mL), and H₂O (180 mL) and allowed to stir for 2 h. 4,4'-Azobis(4-cyanovaleric acid) (0.08 g, 0.29 mmol) was added (63 mol % based on available styrenyl groups), and the reaction mixture was allowed to stir for 0.5 h prior to irradiation for 24 h. During irradiation, the solution changed color from very light green to light yellow. An average diameter of 14 ± 2 nm was obtained from AFM.

SCK 12. This was prepared from **15** (0.24 g, 0.017 mmol) in THF (80 mL), and H₂O (170 mL) and allowed to stir for 1.5 h. 4,4'-Azobis(4-cyanovaleric acid) (0.05 g, 0.19 mmol) was added (85 mol % based on available styrenyl groups), and the reaction mixture was allowed to stir for 0.25 h prior to irradiation for 24 h. During irradiation, the solution changed color from very light green to a light yellow and was turbid with formation of a white precipitate on the sides and bottom of the flask. An average diameter of 19 ± 4 nm was obtained from AFM.

SCK 17. This was prepared from **13** (0.20 g, 0.017 mmol) in THF (60 mL), and H₂O (150 mL) and allowed to stir for 12.75 h. 4,4'-Azobis(4-cyanovaleric acid) (0.02 g, 0.075 mmol) was added (55 mol % based on available styrenyl groups), and the reaction mixture was allowed to stir for 0.75 h prior to irradiation for 24 h. During irradiation, the solution changed color from very light green to yellow and was slightly turbid with some precipitate floating in the solution. After a week, precipitate appeared on the bottom of the storage flask. An average diameter of 18 ± 3 nm was obtained from AFM.

SCK 18. This was prepared from **14** (0.21 g, 0.017 mmol) in THF (60 mL), and H₂O (160 mL) and allowed to stir for 17 h. 4,4'-Azobis(4-cyanovaleric acid) (0.10 g, 0.36 mmol) was added (178 mol % based on available styrenyl groups), and the reaction mixture was allowed to stir for 2 h prior to irradiation for 24 h. During irradiation, the solution changed color from very light green to bright yellow with no evidence of precipitate. After ~10 days some precipitate had formed in the bottom of the storage flask. An average diameter of 16 ± 3 nm was obtained from AFM.

SCK 19. This was prepared from **15** (0.23 g, 0.017 mmol) in THF (70 mL), and H₂O (180 mL) and allowed to stir for 11.5 h. 4,4'-Azobis(4-cyanovaleric acid) (0.05 g, 0.19 mmol) was added (85 mol % based on available styrenyl groups), and the reaction mixture was allowed to stir for 0.5 h prior to irradiation for 24 h. During irradiation, the solution changed color from very light green to light yellow and was turbid with white solid precipitate on the sides of the flask and floating in the solution. An average diameter of 27 ± 5 nm was obtained from AFM.

SCK 20. This was prepared from **16** (0.24 g, 0.017 mmol) in THF (70 mL), and H₂O (170 mL) and allowed to stir for 15.5 h. 4,4'-Azobis(4-cyanovaleric acid) (0.05 g, 0.18 mmol) was added (67 mol % based on available styrenyl groups), and the reaction mixture was allowed to stir for 0.5 h prior to irradiation for 24 h. During irradiation, the solution changed color from very light green to light yellow and was turbid with white solid precipitate on the sides of the flask. An average diameter of 29 ± 2 nm was obtained from AFM.

Bromopoly(ethylene oxide) (1950) Monomethyl Ether (21). Polyethylene glycol monomethyl ether (20.7 g, 0.011 mol, Scientific Polymer Products, MW 1900) was dissolved in THF (35 mL) with application of heat, and then carbon tetrabromide (8.37 g, 0.025 mol)

and triphenylphosphine (6.54 g, 0.025 mol) were added. After 5–10 min of stirring under a N₂ flow, a cloudy white precipitate began to form. The solution was allowed to stir for 0.5 h, and then the THF was removed *in vacuo*. The product was purified by flash column chromatography eluting with CH₂Cl₂ and increasing the polarity to 10% MeOH/CH₂Cl₂ to give **21** as a white solid: yield 18.6 g (88%); ¹H NMR (CDCl₃) δ 3.30 (s, OCH₃), 3.40 (t, *J* = 8 Hz, BrCH₂CH₂), 3.58 (br m, OCH₂CH₂O), 3.74 (t, *J* = 8 Hz, BrCH₂CH₂) ppm. Anal. Calcd for C₈₅H₁₇₁BrO₄₂ (1950): C, 52.49; H, 8.86; Br, 4.11. Found: C, 51.90; H, 8.56; Br, 4.42.

General Procedure for the Quaternization of Polystyrene-*b*-poly(vinylpyridine)-*N*-(chloromethyl)styrene with **21 and Then Cross-Linking To Form the SCK's.** To a 250 mL quartz reaction vessel was added polystyrene-*b*-poly(vinylpyridine)-*N*-(chloromethyl)styrene and an appropriate volume of THF and then H₂O to give a solution concentration between 5 × 10⁻⁵ and 7 × 10⁻⁵ M in a THF:H₂O solvent mixture with a ratio of approximately 1:2.5. The reaction mixture was allowed to stir for 4–6.5 h under a N₂ flow. The functionalized PEO **21** was added, and the mixture was allowed to stir for an additional 11–13 h before 4,4'-azobis(4-cyanovaleric acid) was added (50–80 mol % based available styrenyl groups), and the reaction mixture was allowed to stir for up to 1 h. Irradiation on the open flask was then performed for 24 h within a Rayonet photochemical reactor, which resulted in a decrease in volume due to loss of THF from the heat generated by the lamp. All samples were filtered through a 0.45 μm PTFE filter, and AFM was performed.

PEO-Functionalized SCK 22. To a quartz reaction vessel were added **15** (0.25 g, 0.018 mmol), THF (80 mL), and H₂O (180 mL). The reaction mixture was stirred for 5.5 h under a N₂ flow, **21** (0.26 g, 0.14 mmol, 7.6 equiv) was added, and stirring was continued for 12.25 h. 4,4'-Azobis(4-cyanovaleric acid) (0.05 g, 0.19 mmol) was added (79 mol % based on available styrenyl groups), the reaction mixture was allowed to stir for 0.25 h, and the reaction vessel was then irradiated for 24 h. During irradiation, the solution became slightly yellow in color and was extremely turbid with some precipitate formation. An average diameter of 22 ± 4 nm was obtained from AFM.

PEO-Functionalized SCK 23. To a quartz reaction vessel were added **5** (0.20 g, 0.014 mmol), THF (70 mL), and H₂O (180 mL). The reaction mixture was stirred for 4 h under a N₂ flow, **21** (0.21 g, 0.11 mmol, 7.9 equiv) was added, and stirring was continued for 12 h. 4,4'-Azobis(4-cyanovaleric acid) (0.06 g, 0.22 mmol) was added (50 mol % based on available styrenyl groups), the reaction mixture was allowed to stir for 0.5 h, and the reaction vessel was then irradiated for 20.5 h. The SCK solution was a golden yellow color. An average diameter of 12 ± 2 nm was obtained from AFM.

PEO-Functionalized SCK 24. To a quartz reaction vessel were added **4** (0.25 g, 0.012 mmol), THF (70 mL), and H₂O (180 mL). The reaction mixture was stirred for 5.25 h under a N₂ flow, **21** (0.19 g, 0.10 mmol, 7.9 equiv) was added, and stirring was continued for 12.25 h. 4,4'-Azobis(4-cyanovaleric acid) (0.10 g, 0.36 mmol) was added (54 mol % based on available styrenyl groups), the reaction mixture as allowed to stir for 0.5 h, and the reaction vessel was then irradiated for 24 h. The SCK solution was a golden yellow color. An average diameter of 12 ± 2 nm was obtained from AFM.

Acknowledgment. The authors gratefully acknowledge financial support for this work by a National Science Foundation National Young Investigator Award DMR-9458025 (K.L.W.), Monsanto Company (K.L.W.), a DuPont Young Professor Grant (K.L.W.), and the Office of Naval Research (T.K.). Fellowship support (for K.B.T.) from the Department of Education, Graduate Assistance in Areas of National Need (P200A4014795), is also acknowledged with thanks. The authors are grateful to Dr. M. Afeworki and Professor J. Schaefer for solid state NMR experiments and to Professor P. P. Gaspar for access to the Rayonet photochemical apparatus.

JA9710520